Asian Journal of Chemistry; Vol. 34, No. 8 (2022), 2041-2048

ASIAN JOURNAL OF CHEMISTRY

https://doi.org/10.14233/ajchem.2022.23728

Bis(indolyl)methane and 8-Hydroxyquinoline Derivative based Mixed Ligand Metal Complexes: Synthesis, Characterization, Antimicrobial Screening and Molecular Docking Study

S.S. BORHADE[1,2] and P.T. TRYAMBAKE[1,3,*]

[1]Department of Chemistry, K.T.H.M. College, Nashik-422002, India
[2]Department of Chemistry, S.M.B.S.T. College of Arts, Science and Commerce, Sangamner-422605, India
[3]Department of Chemistry, S.N. Arts, D.J.M. Commerce and B.N.S. Science College, Sangamner-422605, India

*Corresponding author: Tel/Fax: +91 24 25225893; E-mail: pravintryambake21@rediffmail.com

Received: 13 January 2022; *Accepted*: 7 April 2022; *Published online*: 18 July 2022; AJC-20884

Present study described the synthesis of mixed ligand metal complexes of Mn(II), Fe(III), Co(II), Ni(II), Cu(II) and Zn(II). Metal complexes were synthesized by two ligands such as 8-hydroxyquinoline derivative (primary ligand) and *bis*(indolyl)methane derivative (secondary ligand). The ligands and their transition metal complexes were characterized by IR, ^{1}H NMR, mass spectrum, elemental analysis, TGA, electronic spectra (UV) and molar conductance. The results of analysis predicted that both ligands are bidentate and resulting complexes are ML_1L_2 type with molar ratio 1:1:1. To screen their biological potential, the antibacterial and antifungal activity of synthesized compounds have also been investigated. Results of antimicrobial activity were expressed as minimum inhibitory concentration (MIC). Synthesized complexes showed moderate to excellent antimicrobial activity against pathogens. Further, the more potent antimicrobial complexes of Fe(II) and Co(II) were docked with topoisomerase II as a receptor protein, Fe-complex bound to Met1113 (2.53 Å), Asn1296 (2.86 Å) and with nucleotide DC12 (3.28 Å). Similarly, Co-complex bound to Lys1276 (2.27 Å), Leu1280 (2.40 Å), Thr1325 (2.37 Å) and Gly1332 (2.42 Å) *via* intermolecular hydrogen bonding.

Keywords: *Bis*(indolyl)methane, Azo quinoline, Metal complexes, Antimicrobial activity, Molecular docking.

INTRODUCTION

Mixed ligand metal complexes [1] have important applications in various fields such as pharmaceutical [2,3], catalysis [4] as well as phosphorescent materials [5], *etc.* due to this, researchers gave more attention towards the development of more active metal complexes with different ligands. Metal complexes of Mn(II) [6], Fe(III) [6], Co(II) [7], Ni(II) [8], Cu(II) [7], Zn(II) [8] are reported for their enhanced bioactivity.

Derivatives of *bis*(indolyl)methane [9] are the nitrogen-containing important class of heterocyclic compounds with diverse applications in the pharmaceutical field [10]. Particularly *bis*(indolyl)methanes [11] possess biological activities such as antibacterial and insecticidal activities [12], antitumor activity [13], anticonvulsant [13], anticancer agents [14], antifungal [15], anti-inflammatory [16], *etc.* 8-Hydroxyquinoline is also a significant heterocyclic compound with manifold applications in pharmaceutical [17-21]. Moreover, 8-hydroxyquinoline and its derivatives are known for chelating ability [22] as well as their applications in synthesis of different bioactive molecules in the medicinal field [23].

In this study, the synthesis, characterization, molecular docking and biological potential of Mn(II), Fe(III), Co(II), Ni(II), Cu(II) and Zn(II) mixed ligand complexes of 5-((4-chlorophenyl)diazenyl)quinolin-8-ol (ligand 1) and 4-(di(1*H*-indol-3-yl)methyl)benzene-1,2-diol (ligand 2) is reported. Molecular docking study was performed to assess the target for antimicrobial activity. Biological activity study was carried out on two Gram-positive bacteria (*S. aureus* and *S. pyogenus*), two Gram-negative bacteria (*E. coli* and *P. aeruginosa*) and three fungal pathogens (*A. niger*, *C. albicans* and *A. clavatus*).

EXPERIMENTAL

All the purchased chemicals and solvents were of analytical grade reagents (from S.D. Fine Chemicals and Sigma-Aldrich) and used without further purification. By the open capillary method, the melting point of the synthesized ligands and comp-

lexes was determined and uncorrected. Shimadzu FTIR-408 spectrophotometer was used to record the FT-IR spectra in the range between 4000 and 400 cm^{-1} using KBr. In DMF solvent, the conductance was measured using an Equiptronics Conductivity meter (EQ-664A). The ^1H NMR spectra was recorded in DMSO-d_6 at 500 MHz with TMS as an internal standard. Moreover, the LC-MS spectra were recorded on WATER, Q-TOF Micro mass. Elemental analysis was done on Perkin-Elmer EAL240 elemental analyzer. The absorption spectra of the prepared samples were recorded in the wavelength range of 200-800 nm using JASCO V-770ST UV/VIS/NIR spectrophotometer. A thermogravimetric analysis study was done by using a Perkin-Elmer thermogravimetric analyzer at the heating rate of 10 ºC per min in a nitrogen atmosphere.

Synthesis of 5-((4-chlorophenyl)diazenyl)quinolin-8-ol [(L1)]: Ligand 1 (**4**, **Scheme-I**) was synthesized by a known procedure [24].

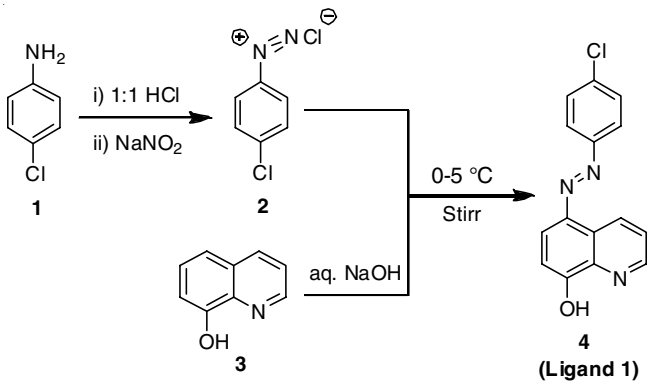

Scheme-I: Preparation of 5-((4-chlorophenyl)diazenyl)quinolin-8-ol (Ligand 1)

Synthesis of 4-(di(1*H*-indol-2-yl)methyl)benzene-1,2-diol [(L2)]: Ligand 2 (**7**, **Scheme-II**) was also synthesized by a procedure as per literature [25]. In brief, a mixture of indole (5, 0.02 mol, 5.85 g) and 3,4-dihydroxy benzaldehyde (6, 0.01 mol, 3.45 g) was taken in a 100 mL round bottom flask. To this solution, 10 mL glacial acetic acid was added and stirred at room temperature (25 ºC) for 3 h. The completion of the reaction was monitored by thin-layer chromatography with mobile phase 15% ethyl acetate in hexane. After completion of the reaction mixture was poured in cold water, separated solid (**7**, ligand 2) was filtered. The crude product was purified by column chromatography using ethyl acetate-hexane solvent. Using an ethyl acetate-hexane solvent, the crude product was purified using column chromatography. FTIR, ^1H NMR, mass spectra and elemental analysis were used to determine the structure. Colour: reddish; Yield: 85%; m.p.: 94-96 ºC; IR (KBr, ν_{max} cm^{-1}): 3408 (-OH, NH), 1607(C=C) 1513, 1455, 1338, 1278, 1095, 875, 745. ^1H NMR (DMSO-d_6, 400 MHz) δ ppm: 5.65 (s, 1H), 6.64 (t, 1H), 6.66 (d, 1H), 6.73 (d, 1H), 6.79 (s, 2H), 6.87 (t, 2H), 7.04 (t, 2H), 7.29 (d, 2H), 7.35 (d, 2H), 8.70 (br. s, 2H), 10.77 (s, 2H) MS: M+1 = 353.3726, Anal. calcd. (found) % for $C_{23}H_{18}N_2O_2$: C, 77.95 (77.20); H, 5.12 (5.01); N, 7.90 (7.35).

Synthesis of metal complex: Ligand 1 (0.01mmol) and ligand 2 (0.01 mmol) and 20 mL ethanol was taken in round bottom flask. The mixture was heated at boiling temperature to make a clear solution. To a above mixture, ethanolic solution of metal chlorides of Mn(II), Fe(II), Co(II), Ni(II), Cu(II) and Zn(II) (0.01 mmol) was added dropwise. The pH of the reaction mixture was maintained to 9-10 with the addition of 0.2 M NaOH solution. The mixture was refluxed with constant stirring for 2.0 h. The separated coloured complex was filtered through Whatman filter paper and washed with ethanol. Finally, the complex was dried in vacuum desiccators over anhydrous $CaCl_2$. The yield was about 80-90% (**Scheme-III**).

Antimicrobial activity: For screening the *in vitro* antimicrobial activity of metal complexes, broth dilution assay was used [26]. For this, two Gram-positive (*Staphylococcus aureus* [MTCC96] and *Streptococcus pyogenus* [MTCC442]) and two Gram-negative (*Escherichia coli* [MTCC443] and *Pseudomonas aeruginosa* [MTCC441]) bacterial strains were used. *Candida albicans* (MTCC 227), *Aspergillus niger* (MTCC 282) and *Aspergillus clavatus* (MTCC 323) were the fungal species used for the antifungal evaluation. The highest dilution yielded results with at least 99% inhibition, which is considered the MIC. Amoxicillin and chloramphenicol were served as positive controls.

Molecular docking: The molecular docking technique was employed using AutoDock4.2 [27] software, to investigate the putative binding mode of most effective antimicrobial metal complexes. For docking, topoisomerase II also referred to as DNA gyrase was used in this study as a receptor protein. DNA gyrase is an important target protein receptor, to explore the binding mode of antibacterial [28] and antifungal [29] compounds. It catalyzes the changes in the DNA strands and is important for replication and bacterial cell survival as it is absent in the eukaryotes. The three-dimensional coordinates of DNA gyrase were collected from the protein database (PDB ID:

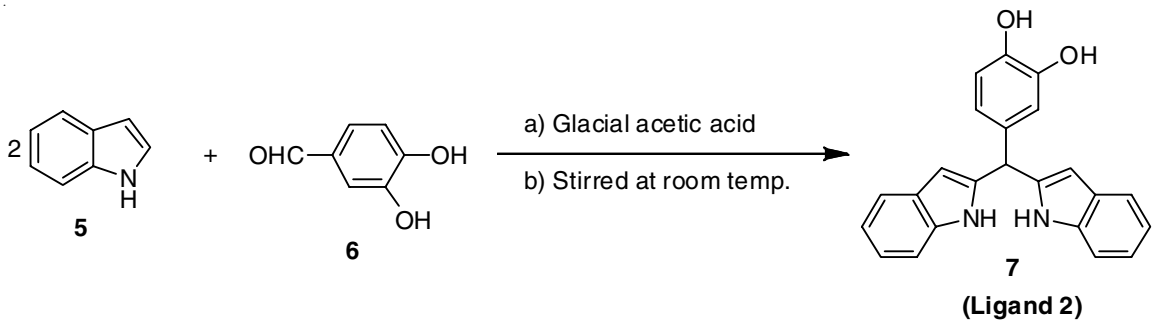

Scheme-II: Preparation of 4-(di(1*H*-indol-2-yl)methyl)benzene-1,2-diol (Ligand 2)

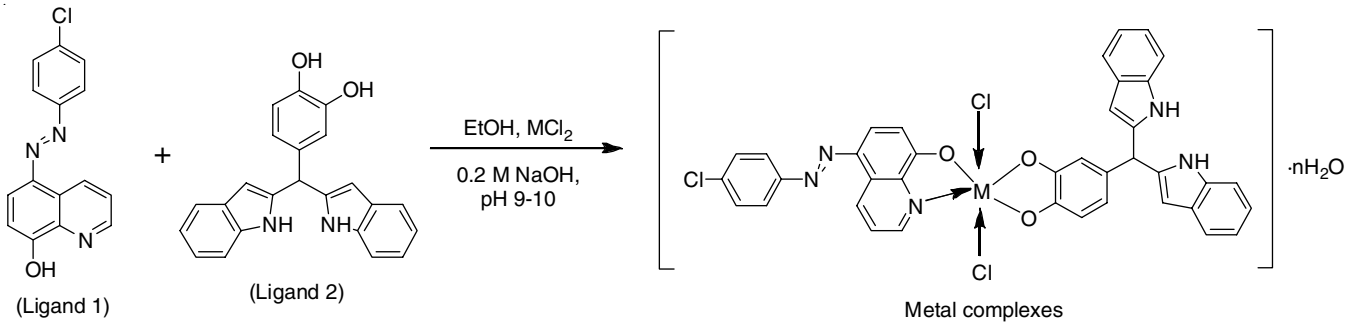

M = Mn(II), Fe(III), Co(II), Ni(II), Cu(II) and Zn(II)

Scheme-III: Structure of metal complex (**3-8**)

2XCT.pdb), which was isolated from *Staphylococcus aureus* [30]. Next, organic metal complexes were built and optimized using the Discovery Studio Visualizer [31]. In this study, the blind and local docking approach were utilized to explore the binding mode and obtained the least energy conformation similar to the earlier study [32]. The active binding mode and analysis of bonding interactions was predicted using PyMol [33] and Chimera [34] software.

RESULTS AND DISCUSSION

The six new mixed ligand metal complexes were synthesized from 5-((4-chlorophenyl)diazenyl)quinolin-8-ol (ligand 1), 4-(di(1*H*-indol-2-yl)methyl)benzene-1,2-diol (ligand 2) with metal chlorides of Mn(II), Fe(III), Co(II), Ni(II), Cu(II), Zn(II) in ethanol.

Elemental analysis: The C,H,N analysis of the ligands and its metal complexes with the molecular formula and the melting points are given in Table-1. The results obtained are in good agreement with those calculated for the suggested molecular formula. It confirms that the composition of metal complexes is ML1L2 (1:1:1).

Molar conductance: The molar conductance values for complexes were determined in DMF as solvent (10^{-3} mol L^{-1}) at room temperature (Table-1). All complexes showed values in the range 1.00 to 4.35 ohm^{-1} cm^2 mol^{-1} indicating the non-electrolytic nature of complexes [35]. This confirms that chloride ions are directly bonded to metal ions [36].

FTIR studies: Both ligands were characterized by FTIR, ^{1}H NMR, mass and elemental analysis. As per spectral analysis of ligand 1, IR spectrum showed absorption peak for different functional groups at 3287 cm^{-1} (-OH), 1506 cm^{-1} (C=N pyridine), 1400 cm^{-1} (N=N linkage), 1289 cm^{-1} (C-O), 1134 cm^{-1} (-Cl) [37]. The IR spectra of ligand 2 showed a major broad absorption peak at 3408 (-OH, NH), peak at 3054 (arom. C-H), 2975 (aliph. C-H), 1607 (C=C), 1278 (C-O) [37]. The mass spectra showed intense peak at 353.3726 (M+1) confirms the formation 4-(di(1*H*-indol-2-yl)methyl)benzene-1,2-diol (ligand 2).

The key vibrational modes of ligand 1 and ligand 2 with transition metal ions are given in Table-2. On examination of IR spectra of ligands and their metal complexes, band at 3408 cm^{-1} in ligand-2 due to hydroxyl groups is disappeared on complexation indicated the association of oxygen atoms is in coordination with the metal ion. Also, the coordination of azo 8-hydroxyquinoline (ligand 1) with metal ion was supported by the disappearance of band at 3287 cm^{-1} due to hydroxyl group. This confirms the formation of C-O-M bonding in complexes. Moreover, shifting of frequency for C=N band of quinoline ring in ligand 1 from 1571 cm^{-1} to lower frequency. The strong band in ligand 1 and ligand 2 at 1289 cm^{-1} and 1278 cm^{-1}, respectively due to C-O bond, in all metal complexes this frequency has shifted to lower frequencies in between 1270-1249 cm^{-1}. This also confirms the formation of C-O-M bonding in the metal complexes. Broad band in all the synthesized complexes around 3461-3426 cm^{-1} confirmed the presence of coordinated water molecules. The two new bands at 518-476 cm^{-1} and 477-424 cm^{-1} confirmed the M-O and M-N bonding in present metal complexes [37].

NMR studies: In ^{1}H NMR spectra, a broad singlet at δ 11.11 ppm confirmed the presence of –OH group, chemical shift values in δ 7.26 to 9.33 ppm confirmed the formation of azo-linkage with nine aromatic protons. The mass spectra showed

TABLE-1
PHYSICAL PARAMETERS OF LIGANDS AND ITS METAL COMPLEXES

Compounds	Colour	m.w.	Yield (%)	m.p. (°C)	Molar cond.	Elemental analysis (%): Found (calcd.)		
						C	H	N
Azo quinoxaline (L1)	Brown	284.0800	89	216-218	–	63.20 (63.50)	3.42 (3.55)	14.78 (14.81)
Bis(indolyl)methane (L2)	Reddish	353.3726	85	94-96	–	77.20 (77.95)	5.01 (5.12)	7.35 (7.90)
$Mn(L1)(L2)Cl_2·3H_2O$	Reddish brown	814.6215	83	250<	1.00	55.89 (56.00)	3.74 (3.83)	8.59 (8.59)
$Fe(L1)(L2)Cl_2·5H_2O$	Reddish brown	850.5231	80	250<	1.98	53.42 (53.57)	4.08 (4.14)	8.20 (8.22)
$Co(L1)(L2)Cl_2·H_2O$	Reddish brown	786.6018	82	250<	4.01	58.21 (58.29)	3.43 (3.48)	8.89 (8.94)
$Ni(L1)(L2)Cl_2·2H_2O$	Brown	808.6449	85	250<	4.35	56.92 (57.00)	3.58 (3.65)	8.66 (8.75)
$Cu(L1)(L2)Cl_2·2H_2O$	Brown	808.6587	83	250<	3.98	56.57 (56.66)	3.58 (3.63)	8.61 (8.69)
$Zn(L1)(L2)Cl_2·H_2O$	Reddish brown	786.6290	85	250<	2.73	57.77 (57.82)	3.38 (3.45)	8.78 (8.87)

TABLE-2
CHARACTERISTIC INFRARED ABSORPTION BANDS (cm^{-1}) OF THE LIGANDS AND THEIR METAL COMPLEXES

Compounds	Co-ordinated water	ν(-OH)	Phenolic C-O	ν(Py.N)	ν(M-O)	ν(M-N)
Azo quinoxaline (L1)	–	3287	1289	1571	–	–
Bis(indolyl)methane (L2)	–	3408	1278	–	–	–
$Mn(L1)(L2)Cl_2 \cdot 3H_2O$	3461	–	1270	1555	517	447
$Fe(L1)(L2)Cl_2 \cdot 5H_2O$	3432	–	1264	1563	516	453
$Co(L1)(L2)Cl_2 \cdot H_2O$	3448	–	1250	1527	497	426
$Ni(L1)(L2)Cl_2 \cdot 2H_2O$	3456	–	1250	1563	476	424
$Cu(L1)(L2)Cl_2 \cdot 2H_2O$	3442	–	1249	1562	496	426
$Zn(L1)(L2)Cl_2 \cdot H_2O$	3426	–	1251	1568	518	477

an intense peak at 284.08 (M+1) confirms the formation of 5-((4-chlorophenyl)diazenyl)quinolin-8-ol (ligand 1).

The ^{1}H NMR spectra showed broad singlet at δ 8.70 and 10.77 ppm confirmed the presence of –OH and -NH- groups, a singlet at δ 5.65 ppm represents the aliphatic hydrogens while chemical shift values in δ 6.64 to 7.35 ppm showed aromatic hydrogens.

Mass spectra of complexes: Mass spectra of mixed ligands metal complexes (**3-8**) showed molecular ion peaks corresponding to newly synthesized complexes and molecular weight of unstable fragments may be due to degradation of target metal complex and collision of ions. Molecular ion peak and mass of various fragments of metal complexes confirm the stoichiometry of metal chelates as [ML1L2] type. Mass spectra of Zn-complex is shown in Fig. 1.

Thermal studies: To understand the stability and decomposition, thermogravimetric analysis of all the mixed ligands metal complexes was carried out in the temperature range of 25-800 ºC with a heating rate of 10 ºC min^{-1} in a N_2 atmosphere and results are given in Table-3. The TGA cure of Co-complex and Cu-complex are given in Fig. 2. The loss in weight is due to the role of temperature. As per the thermogram, all the metal

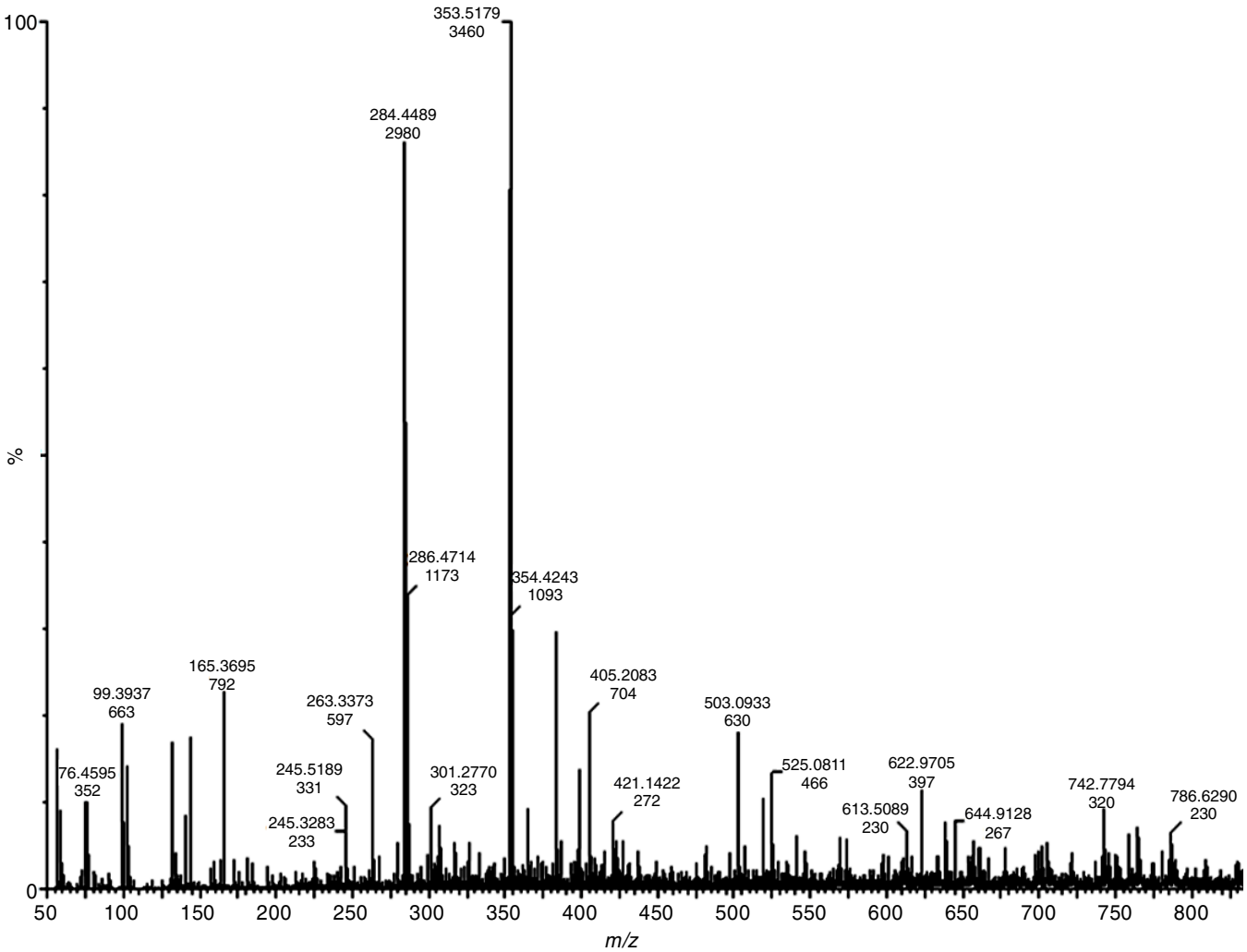

Fig. 1. Mass spectra of Zn complex

TABLE-3
THERMAL DATA FOR MIXED LIGAND METAL COMPLEXES (**1-6**)

Complex	Temperature range (°C)	Weight loss (%)		Assigned dec. product
		Found	Expected	
$Mn(L1)(L2)Cl_2·3H_2O$	85-220	16.2	15.4	2Cl, $3H_2O$
	230-435	59.6	60.2	Organic part of ligands
$Fe(L1)(L2)Cl_2·5H_2O$	80-200	18.58	18.94	2Cl, $5H_2O$
	230-435	58.4	59.8	Organic part of ligands
$Co(L1)(L2)Cl_2·H_2O$	80-190	12.29	11.32	2Cl, H_2O
	240-450	67.35	68.28	All remaining organic part
$Ni(L1)(L2)Cl_2·2H_2O$	80-220	13.77	13.24	2Cl, $2H_2O$
	260-467	63.45	64.55	All remaining organic part
$Cu(L1)(L2)Cl_2·2H_2O$	80-225	13.72	13.29	2Cl, $2H_2O$
	260-467	63.61	64.29	All remaining organic part
$Zn(L1)(L2)Cl_2·H_2O$	50-180	11.56	11.30	2Cl, H_2O
	230-486	66.90	67.78	All remaining organic part

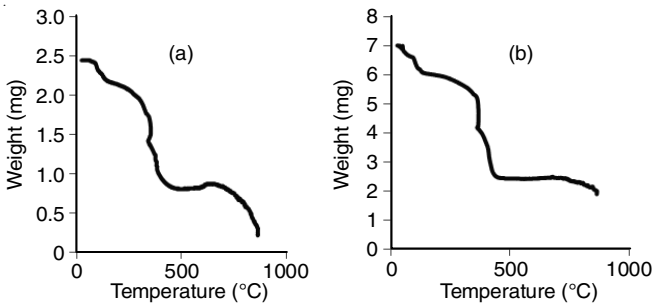

Fig. 2. TGA of (a) Co complex and (b) Cu complex

complexes were decomposed in two steps. The first decomposition occurs between 100-200 ºC with an exothermic peak at 225-800 ºC, exhibited a weight loss of 11-18%. It may lose water molecules and chloride ions. Further, in second step, the continuous and rapid loss in weight takes place above 230 ºC, which represents the complete decomposition of the mixed ligands metal complexes. It exhibiting weight loss of around 65 to 70%. Leaving behind metal residue and carbon around 15-20%.

Electronic spectra: The UV-visible spectra of ligands and its metal complexes were recorded in DMF at 298 K and data is tabulated in Table-4. The electronic spectrum of the free ligand 1 shows absorption at 236, 255 nm and 269, 400 nm due to π-π* and n-π* transitions, respectively while ligand 2 shows absorption at 240, 255 and 262, 298 nm due to π-π* and n-π* transitions, respectively. An intense absorption band for all the metal complexes observed in the range 226-255 nm is due to π-π* transitions in the aromatic units and bands at 269-274 nm region are due to n-π* transitions of all the complexes (Fig. 3) [38]. A band in the region of 477-525 nm is due to the LMCT transition [39]. Mn(II) complex showed an absorption band at 521 nm is assigned to the $^6A_{1g}\rightarrow{}^4T_{2g}$ transition for a distorted octahedral Mn(II) complex. Co(II) complex showed an absorption band at 377 and 459 nm are assigned to the $^4T_{1g}(F)\rightarrow{}^4A_{2g}(F)$ and $^4T_{1g}(F)\rightarrow{}^4T_{1g}(P)$ transitions for a distorted octahedral geometry of the complex [40]. The Ni(II) complex shows a *d-d* band at 514 nm due to $^3A_{2g}(F)/{}^3T_{1g}(P)$ transition, which corresponds to the octahedral geometry [40]. The diffuse electronic spectrum of Cu complex contains

TABLE-4
ELECTRONIC SPECTRAL DATA OF THE LIGANDS AND THEIR COMPLEXES

Compounds	π-π*	n-π*	*d-d* transition
Azo quinoxaline (L1)	236, 255	269, 400	–
Bis(indolyl)methane (L2)	255, 262	298, 416, 504	–
$Mn(L1)(L2)Cl_2·3H_2O$	240, 262	269, 348	521
$Fe(L1)(L2)Cl_2·5H_2O$	242	269	525
$Co(L1)(L2)Cl_2·H_2O$	226, 255	270	477
$Ni(L1)(L2)Cl_2·2H_2O$	230, 240	256, 274	514
$Cu(L1)(L2)Cl_2·2H_2O$	226, 240	255, 268	447
$Zn(L1)(L2)Cl_2·H_2O$	235, 239	254, 271, 348	–

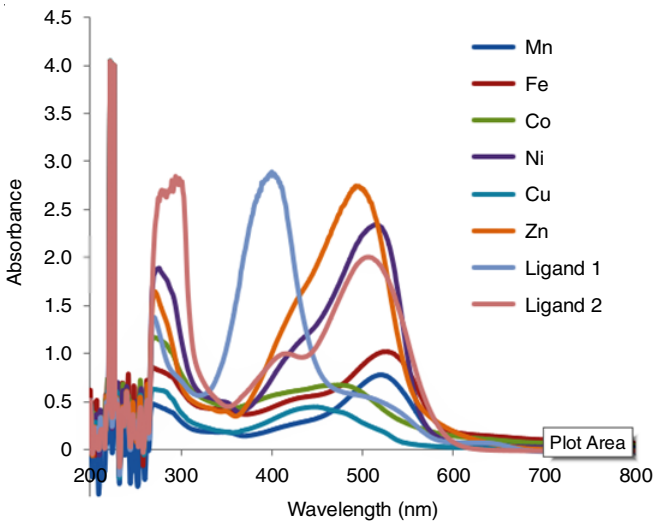

Fig. 3. UV-visible spectra of mixed ligands and its metal complexes

two broad bands at approximately 355 and 447 nm, attributed to the $^2E_g\rightarrow{}^2T_{2g}$ transition and to charge transfer, respectively. This proposes a distorted octahedral structure of the complex [41]. Moreover, the Zn(II) complex exhibited charge transfer transitions (LMCT) at 492 nm [42].

Antibacterial activity: All the synthesized mixed ligands metal complexes compounds possess good antimicrobial activity against all the studied microorganisms. The *in vitro* screening and evaluation results (minimum inhibitory concentration) against the studied microorganisms are tabulated in Table-5.

TABLE-5
ANTIMICROBIAL ACTIVITIES OF SYNTHESIZED COMPOUNDS

Compound	MIC values (µg/mL)						
	Antibacterial activity				Antifungal activity		
	E. coli (MTCC443)	*P. aeruginosa (MTCC441)*	*S. aureus* (MTCC96)	*S. pyogenes (MTCC442)*	*C. albicans* MTCC 227	*A. niger* MTCC282	*A. clavatus* MTCC1323
Azo quinoxaline (L1)	125	250	125	125	500	1000	1000
Bis(indolyl)methane (L2)	125	250	250	200	500	1000	500
$Mn(L1)(L2)Cl_2{\cdot}3H_2O$	250	100	100	125	250	250	250
$Fe(L1)(L2)Cl_2{\cdot}5H_2O$	62.5	100	200	50	200	200	250
$Co(L1)(L2)Cl_2{\cdot}H_2O$	100	100	250	100	250	500	500
$Ni(L1)(L2)Cl_2{\cdot}2H_2O$	250	100	100	125	250	500	1000
$Cu(L1)(L2)Cl_2{\cdot}2H_2O$	200	200	100	100	200	500	500
$Zn(L1)(L2)Cl_2{\cdot}H_2O$	100	125	200	100	500	250	250
Ampicillin	100	100	250	100	–	–	–
Chloramphenicol	50	50	50	50	–	–	–
Greseofulvin	–	–	–	–	500	100	100

Metal complexes showed a better activity against most of the bacterial pathogens than both ligands. With regard to the activity against *E. coli*, complexes **4**, **5** and **8** exhibited the excellent activity, which is equally or more potent than ampicillin (100 µg/mL) but 50% less active than chloramphenicol. Complex **4** which is an iron complex showed excellent activity 62.5 µg/mL as compared to ampicillin (100 µg/mL) while complexes **3**, **6** and **7** as well as both ligands showed the moderate activity against *E. coli*. Furthermore, all complexes showed activity against *P. aeruginosa*, but complexes **3**, **4**, **5**, **6** are equally potent as ampicillin (100 µg/mL) while complexes **7** and **8** both showed the moderate activity. Moreover, all the complexes showed activity against *S. aureus*, but complexes **3**, **6**, **7** are equally potent as standard drug ampicillin while complexes **4**, **5**, **7** and both ligands showed the moderate activity. Finally, complex **4** (50 µg/mL) showed an excellent activity against bacterial stain *S. pyogenus* like concentration as compared to both standard drugs while other complexes possess a good activity.

Antifungal activity: Three fungal stains such as *Candida albicans*, *Aspergillus niger*, *Aspergillus clavatus* were used to study the antifungal activity of the synthesized ligands and its mixed ligand metal complexes. The results are shown in Table-5. The results of synthesized compounds were compared with the standard drug griseofulvin. Antifungal data showed that all the reported analogs are potentially active against *C. albicans*. Complexes **3** to **7** showed excellent activity (200-250 µg/mL) to griseofulvin. Moreover, all complexes showed the moderate inhibition efficiency against the other two pathogens.

Molecular docking: Molecular docking was employed to investigate the binding mode of antibacterial compounds (Table-6) using AutoDock4.2. The least energy docked conformation of antibacterial compounds with DNA gyrase receptor were found to be -13.22, -12.75 kcal/mol for Fe and Co complex, respectively (Fig. 4). The docking study reveals that both these antibacterial compounds prefer to binds at the interface of DNA and gyrase protein and show significant binding affinities as shown in Table-6. Further, the hydrogen bonding interaction analysis shows that all these antibacterial compounds form bonding interactions with the protein and DNA base pairs as shown in Fig. 5.

TABLE-6
BONDING INTERACTION OF Fe AND Co COMPLEXES WITH DNA GYRASE RECEPTOR, ENERGY VALUES (kcal/mol)

Metal complexes	Binding energy	Atoms involved in bonding	Distance atom pair	Angle
Fe	-13.22	Met1113-CH···Cl-Drug	2.53	142.64
		Asn1296-N···HC-Drug	2.86	121.59
		DC12-N··· HC-Drug	3.28	137.23
Co	-12.75	DC-O3···HC-Drug	2.23	161.61
		Lys1276-O···HC-Drug	2.27	134.24
		Leu1280-CH···F-Drug	2.40	155.46
		Thr1325-N···HN-Drug	2.37	145.03
		Gly1332-N···HN-Drug	2.42	126.51

The molecular docking analysis of DNA gyrase with Fe complex shows the bonding interactions with the residues such as Met1113 (2.53 Å), Asn1296 (2.86 Å) and with nucleotide DC12 (3.28 Å) as shown in Fig. 5a. Similarly, the DNA gyrase and Co-complex are stabilized by the bonding interactions with base-pair DC (2.23 Å) and gyrase residues such as Lys1276 (2.27 Å), Leu1280 (2.40 Å), Thr1325 (2.37 Å) and Gly1332 (2.42 Å) as shown in Fig. 5b.

Overall, the molecular docking study revealed that the synthesized Fe and Co complexes are stabilized by hydrogen bonding interactions and forms a stable complex with the DNA gyrase with reasonable binding energy. Hence, this may inhibit the DNA gyrase activity further to stop the catalyze changes in the DNA topology and induces cell apoptosis that leads to cell death.

Conclusion

In present study, synthesis of azo-quinoline derivative (ligand 1), *bis* indole derivative (ligand 2) and its mixed ligand metal complexes of Mn(II), Fe(III), Co(II), Ni(II), Cu(II), Zn(II) metal ion were reported. Various spectroscopic techniques were used to demonstrate the structure, nature of bonding and stoichiometry of complexes. Metals bind through three oxygen, one nitrogen, two ligands and chloride, with water molecules present in the coordination sphere. The antimicrobial activity of metal complexes ranged from moderate to excellent. Metal complexes Fe, Co and Zn were found to be effective against

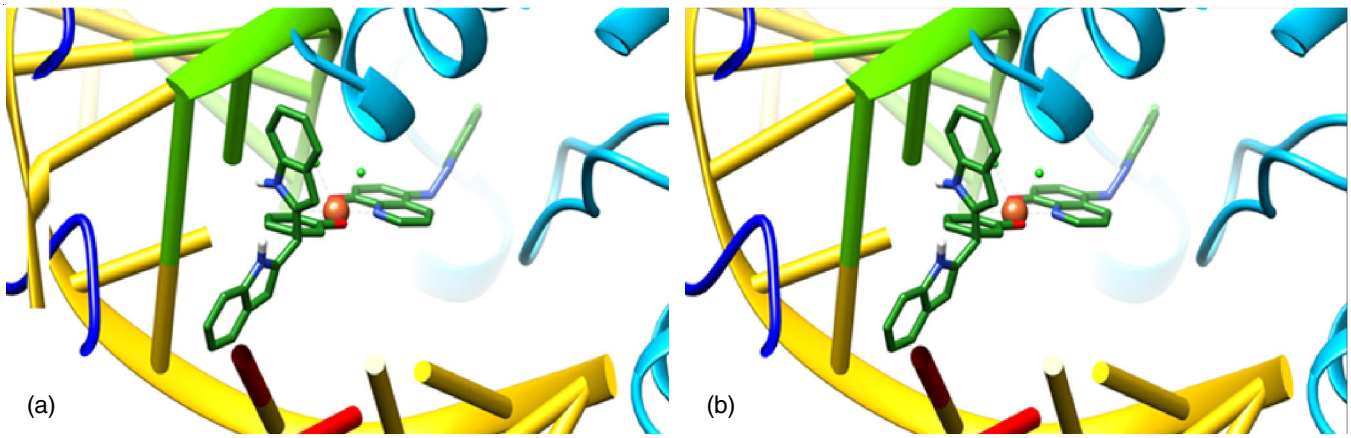

Fig. 4. Binding mode of Fe complex (a) and Co complex (b) with DNA gyrase

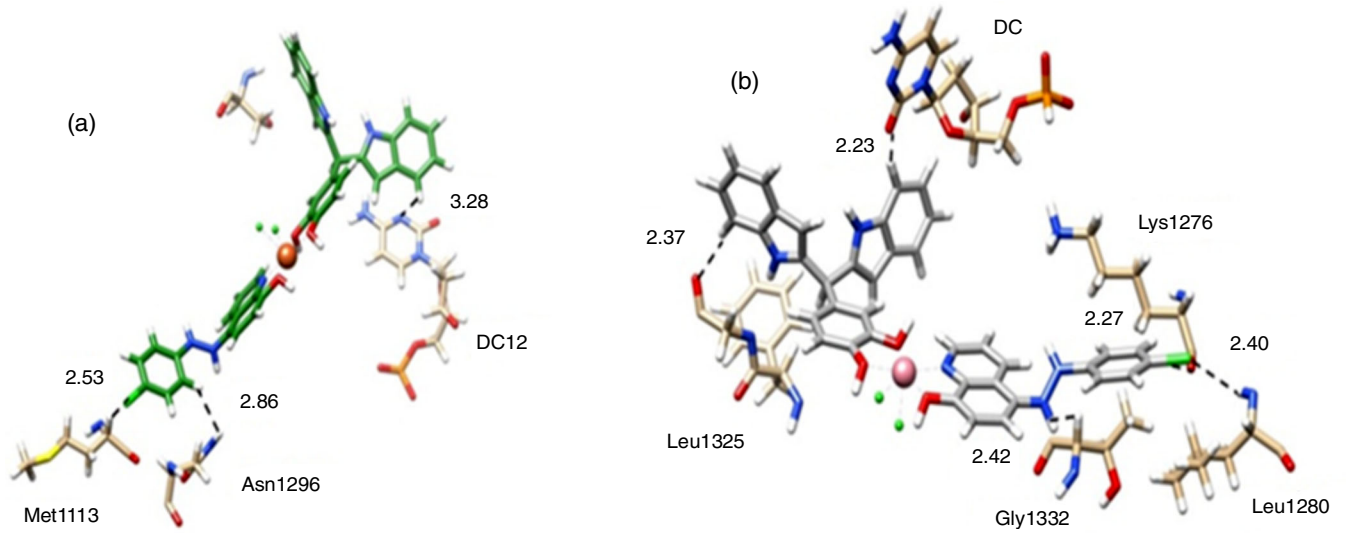

Fig. 5. Interactions of (a) Fe complex and (b) Co complexes with DNA gyrase. The images of 3D interactions of DNA gyrase with derivatives are visualized using the Chimera

all the studied bacterial strains. The Mn-complex was found to have significant activity against all fungal stains, while the other complexes were found to have significant activity against *Candida albicans*. The more potentially bioactive Fe and Co complexes were computationally investigated by use of molecular docking simulation with DNA gyrase. The molecular docking study revealed that the synthesized Fe and Co complexes were stabilized by hydrogen bonding interactions and forms a stable complex with the DNA gyrase with reasonable binding energy.

ACKNOWLEDGEMENTS

The authors are grateful to Principal, KTHM College, Nashik for support and providing a laboratory facility as well as providing TGA-DTA analysis facility. Authors are thankful to the Punjab University Chandigarh for providing FTIR, CHN analysis, NMR and ESI-Mass spectra.

CONFLICT OF INTEREST

The authors declare that there is no conflict of interests regarding the publication of this article.

REFERENCES

1. N. Raman, S. Sobha and M. Selvaganapathy, *Monatsh. Chem.*, **143**, 1487 (2012); https://doi.org/10.1007/s00706-012-0718-4
2. W. Ahmad, S.A. Khan, K.S. Munawar, A. Khalid and S. Kawanl, *Trop. J. Pharm. Res.*, **16**, 1137 (2017); https://doi.org/10.4314/tjpr.v16i5.23
3. B. Duff, V. Reddy Thangella, B.S. Creaven, M. Walsh and D.A. Egan, *Eur. J. Pharmacol.*, **689**, 45 (2012); https://doi.org/10.1016/j.ejphar.2012.06.004
4. S.Y. Ebrahimipour, Z.R. Ranjabr, E.T. Kermani, B.P. Amiri, H.A. Rudbari, A. Saccá and F.A. Hoseinzade, *Transition Met. Chem.*, **40**, 39 (2015); https://doi.org/10.1007/s11243-014-9887-9
5. N. Okamura, T. Nakamura, S. Yagi, T. Maeda, H. Nakazumi, H. Fujiwara and S. Koseki, *RSC Adv.*, **6**, 51435 (2016); https://doi.org/10.1039/C6RA09385J
6. T.T. Al-Nahary, *J. Saudi Chem. Soc.*, **13**, 253 (2009); https://doi.org/10.1016/j.jscs.2009.10.004
7. D. Avci, S. Altürk, F. Sönmez, Ö. Tamer, A. Basoglu, Y. Atalay, B.Z. Kurt and N. Dege, *J. Mol. Struct.*, **1197**, 645 (2019); https://doi.org/10.1016/j.molstruc.2019.07.039
8. P.P. Utthra, G. Kumaravel and N. Raman, *J. Mol. Struct.*, **1150**, 374 (2017); https://doi.org/10.1016/j.molstruc.2017.09.002
9. G.W. Gribble, *J. Chem. Soc. Perkin Trans. I*, 1045 (2000); https://doi.org/10.1039/a909834h

10. R.J. Sundberg, The Chemistry of Indoles, Academic Press: New York (1970).
11. T. Pillaiyar, M. Dawood, H. Irum and C.E. Müller, *ARKIVOC*, 1 (2018); https://doi.org/10.24820/ark.5550190.p010.259
12. M. Lounasmaa and A. Tolvanen, *Nat. Prod. Rep.*, **17**, 175 (2000); https://doi.org/10.1039/a809402k
13. A. Andreani, S. Burnelli, M. Granaiola, A. Leoni, A. Locatelli, R. Morigi, M. Rambaldi, L. Varoli, L. Landi, C. Prata, M.V. Berridge, C. Grasso, H.-H. Fiebig, G. Kelter, A.M. Burger and M.W. Kunkel, *J. Med. Chem.*, **51**, 4563 (2008); https://doi.org/10.1021/jm800194k
14. A. Bahuguna, A. Singh, P. Kumar, D. Dhasmana, V. Krishnan and N. Garg, *Comput. Biol. Med.*, **116**, 103574 (2020); https://doi.org/10.1016/j.compbiomed.2019.103574
15. A. Kamal, M.N.A. Khan, K. Srinivasa Reddy, Y.V.V. Srikanth, S. Kaleem Ahmed, K. Pranay Kumar and U.S.N. Murthy, *J. Enzyme Inhib. Med. Chem.*, **24**, 559 (2009); https://doi.org/10.1080/14756360802292974
16. M. Shiri, M.A. Zolfigol, H.G. Kruger and Z. Tanbakouchian, *Chem. Rev.*, **110**, 2250 (2010); https://doi.org/10.1021/cr900195a
17. B.S. Hurlbert, R. Ferone, T.A. Herrmann, G.H. Hitchings, M. Barnett and S.R.M. Bushby, *J. Med. Chem.*, **11**, 711 (1968); https://doi.org/10.1021/jm00310a017
18. X. Mao, X. Li, R. Sprangers, X. Wang, A. Venugopal, T. Wood, Y. Zhang, D.A. Kuntz, E. Coe, S. Trudel, D. Rose, R.A. Batey, L.E. Kay and A.D. Schimmer, *Leukemia*, **23**, 585 (2009); https://doi.org/10.1038/leu.2008.232
19. J.M. Singh, *J. Med. Chem.*, **13**, 1018 (1970); https://doi.org/10.1021/jm00299a066
20. L.F. Miller and R.E. Bambury, *J. Med. Chem.*, **15**, 415 (1972); https://doi.org/10.1021/jm00274a023
21. N.T. Huy, D.T. Uyen, A. Maeda, D.T.X. Trang, T. Oida, S. Harada and K. Kamei, *Antimicrob. Agents Chemother.*, **51**, 350 (2007); https://doi.org/10.1128/AAC.00985-06
22. V. Prachayasittikul, V. Prachayasittikul, S. Prachayasittikul and S. Ruchirawat, *Drug, Des. Devel. Ther.*, **7**, 157 (2013); https://doi.org/10.2147/DDDT.S49763
23. Z.H. Khalil, A.A. Abdel-Hafez, A.A. Geies and A.M. Kamal El-Dean, *Bull. Chem. Soc. Jpn.*, **64**, 668 (1991); https://doi.org/10.1246/bcsj.64.668
24. S.S. Borhade and P.T. Tryambake, *Asian J. Chem.*, **33**, 885 (2021); https://doi.org/10.14233/ajchem.2021.23110
25. M. El-Sayed, K. Mahmoud and A. Hilgeroth, *Curr. Chem. Lett.*, **3**, 7 (2014); https://doi.org/10.5267/j.ccl.2013.10.003
26. I. Wiegand, K. Hilpert and R.E.W. Hancock, *Nat. Protoc.*, **3**, 163 (2008); https://doi.org/10.1038/nprot.2007.521
27. G.M. Morris, R. Huey, W. Lindstrom, M.F. Sanner, R.K. Belew, D.S. Goodsell and A.J. Olson, *J. Comput. Chem.*, **30**, 2785 (2009); https://doi.org/10.1002/jcc.21256
28. A. Hussain, M.A. Rather, M.S. Dar, N.A. Dangroo, M.A. Aga, A. Qayum, A.M. Shah, Z. Ahmad, M.J. Dar and Q.P. Hassan, *Microbiol. Res.*, **207**, 196 (2018); https://doi.org/10.1016/j.micres.2017.12.004
29. D. Steverding, P. Evans, L. Msika, B. Riley, J. Wallington and S. Schelenz, *Med. Mycol.*, **50**, 333 (2012); https://doi.org/10.3109/13693786.2011.609186
30. B.D. Bax, P.F. Chan, D.S. Eggleston, A. Fosberry, D.R. Gentry, F. Gorrec, I. Giordano, M.M. Hann, A. Hennessy, M. Hibbs, J. Huang, E. Jones, J. Jones, K.K. Brown, C.J. Lewis, E.W. May, M.R. Saunders, O. Singh, C.E. Spitzfaden, C. Shen, A. Shillings, A.J. Theobald, A. Wohlkonig, N.D. Pearson and M.N. Gwynn, *Nature*, **466**, 935 (2010); https://doi.org/10.1038/nature09197
31. BIOVIA Discovery Studio Modeling Environment, Release 2017, San Diego (2016).
32. A. Rai, T.K. Gupta, S. Kini, A. Kunwar, A. Surolia and D. Panda, *Biochem. Pharmacol.*, **86**, 378 (2013); https://doi.org/10.1016/j.bcp.2013.05.024
33. W.L. DeLano, The PyMOL Molecular Graphics System, Version 1.1, Schrödinger LLC (2002).
34. E.F. Pettersen, T.D. Goddard, C.C. Huang, G.S. Couch, D.M. Greenblatt, E.C. Meng and T.E. Ferrin, *J. Comput. Chem.*, **25**, 1605 (2004); https://doi.org/10.1002/jcc.20084
35. Z.H. Chohan and M. Praveen, *Appl. Organomet. Chem.*, **15**, 617 (2001); https://doi.org/10.1002/aoc.179
36. F.A. El-Saied, T.A. Salem, M.M.E. Shakdofa, A.N. Al-Hakimi and A. Radwan, *Beni-Suef Univ. J. Basic Appl. Sci.*, **7**, 420 (2018); https://doi.org/10.1016/j.bjbas.2017.09.002
37. K.D. Patel and H.S. Patel, *Arab. J. Chem.*, **10**, S1328 (2017); https://doi.org/10.1016/j.arabjc.2013.03.019
38. S. Indira, G. Vinoth, M. Bharathi and K.S. Bharathi, *J. Mol. Struct.*, **1198**, 126886 (2019); https://doi.org/10.1016/j.molstruc.2019.126886
39. D. Cremer and J.A. Pople, *J. Am. Chem. Soc.*, **97**, 1354 (1975); https://doi.org/10.1021/ja00839a011
40. A.S.A. Zidan, A.I. El-Said and M.S. El-Meligy, *J. Therm. Anal. Calorim.*, **62**, 665 (2000); https://doi.org/10.1023/A:1026761007006
41. D.P. Singh, R. Kumar, V. Malik and P. Tyagi, *Transition Met. Chem.*, **32**, 1051 (2007); https://doi.org/10.1007/s11243-007-0279-2
42. P. Bharati, A. Bharti, M.K. Bharty, S. Kashyap, U.P. Singh and N.K. Singh, *Polyhedron*, **63**, 222 (2013); https://doi.org/10.1016/j.poly.2013.07.027